第36卷第5期
2017年10月

红外与毫米波学报
J. Infrared Millim. Waves

Vol. 36, No.5
October, 2017

文章编号: 1001-9014(2017)05-0526-08

DOI:10.11972/j.issn.1001-9014.2017.05.003

118 GHz single pole double throw switches using filter synthesis method

YAO Chang-Fei[1], CHEN Zhen-Hua[1], GE Jun-Xiang[1], ZHOU Ming[2], WEI Xiang[2]

(1. School of Electronic and Information Engineering, Nanjing University of Information Science and Technology, Nanjing 210044, China;
2. Department of Microwave and Millimeter Wave Modules, Nanjing Electronic Devices Institute. Nanjing, 210016, China)

Abstract: 118 GHz single pole double throw (SPDT) switches were designed and tested for radiometers in satellite applications. Filter synthesis method was proposed for the switches analysis. Based on equivalent circuit of the discrete AlGaAs/GaAs heterojunction PIN diodes, lumped element filter model of the switches was synthesized and its equivalent distributed circuit was developed. The size of the developed 118 GHz quasi-MMIC SPDT switch circuit is $6 \times 2.5 \times 0.1$ mm^3. For the packaged SPDT switch module, insertion loss (IL) introduced by mounting deviation of the waveguide microstrip transitions and the bonded ribbons is discussed. In the frequency range 110 ~ 120 GHz, the IL of the switch modules is less than 3.0 dB and typical value is 2.6 dB, and their isolation is higher than 22 dB. Response time, switch on time, switch off time and recovery time of the switches are lower than 18 ns, 20 ns, 10 ns and 18 ns, respectively. The 118 GHz switches can be widely used in transceiver systems.

Key words: SPDT switch, PIN diode, insertion loss, isolation
PACS: 07. 50. Ek

基于滤波器综合分析法的118 GHz单刀二掷开关

姚常飞[1], 陈振华[1], 葛俊祥[1], 周 明[2], 魏 翔[2]

(1.南京信息工程大学 电子与信息工程学院,江苏 南京 210044;
2.南京电子器件研究所 微波毫米波模块电路事业部,江苏 南京 210016)

摘要:采用滤波器综合分析方法,基于分立式AlGaAs/GaAs异质结PIN二极管,根据其等效寄生参数,综合出单刀二掷开关集总参数滤波器模型,以此分析其等效分布参数电路,设计出了118 GHz星载辐射计用单刀二掷开关准单片,开关电路尺寸$6 \times 2.5 \times 0.1$ mm^3.通过开关模块封装用波导-微带过渡和键合金带插损的分析研究,研制出了低插损的118 GHz开关模块,在110~120 GHz,测得开关插损小于3.0 dB,插损典型值2.6 dB;开关隔离度大于22 dB;开关响应时间、导通时间、关断时间、恢复时间分别小于18 ns、20 ns、10 ns、18 ns,该准单片作为通道切换开关可集成应用于118 GHz收发组件中.

关 键 词:单刀二掷开关;PIN二极管;插损;隔离度

中图分类号:TN451 **文献标识码**:A

Recently, with the progress of MMIC technology, solid state switches are widely used in microwave and millimeter wave radars, electronic warfare (EW) and communication systems. Millimeter-wave radiometers at 60 GHz, 89 GHz and 118 GHz commonly need a SPDT for channel switching between the receiver and the integrated calibration terminal. In order to reduce the size and lower the cost of millimeter-wave systems, it is important that the switches may be integrated with subsequent front-end components. Being the first component connected between the antenna and the receiver front-end, high IL of the millimeter wave band SPDT switches can greatly affect the receivers' sensitivity. Therefore, for such applications, low IL is required. In order to realize a low IL SPDT switch, especially for the frequency above 100 GHz, the parasitic parameters of the device chips arise as a limiting factor. The switching devices must have the characteristics of high switching cutoff frequency, and minimum number of diodes for low IL while the switch isolation requirement is fulfilled. In recent

Received date: 2017-03-20, **revised date**: 2017-07-08 **收稿日期**:2017-03-20, **修回日期**:2017-07-08
Foundation items: Jiangsu Innovation & Entrepreneurship Group Talents Plan
Biography: YAO Chang-fei (1982-), male, Changzhou, Jiangsu Province, China, Ph. D. Research fields include Millimeter wave and Submillimeter wave circuit and systems. E-mail: yaocf1982@163.com

decades, many monolithic millimeter wave GaAs PIN diode and HEMT switch chips were reported[1-11]. These switches demonstrated good performance with both low IL and high isolation. However, commercial MMIC switches are not always available for system integration while operation frequency is higher than 100 GHz. Microstrip hybrid MIC switches employing discrete diodes can achieve high performance and low cost while MMIC chips are impossible to get easily. Recently, many papers have demonstrated that the switches were commonly realized with low cost Si CMOS and SiGe BiCMOS technology, and they had shown high performance in W-band and D-band frequencies[12-17].

In this paper, low IL 118 GHz quasi-MMIC SPDT switches are designed and tested. Under forward bias, the shunt connected AlGaAs/GaAs heterojunction PIN diode provides a low on-state series resistance path to ground for high isolation. Under reverse bias, the RF junction capacitance of the PIN diodes is very low, while the IL of the switches is unaffected. Based on equivalent circuit parameters of the discrete diodes, lumped element filter model of the switches is synthesized and its equivalent distributed circuit is developed. The circuit size is $6 \times 2.5 \times 0.1$ mm^3. In the frequency from 110 to 120 GHz, the measured IL of the packaged SPDT switch modules is less than 3.0 dB, typical IL is 2.6 dB, and isolation is higher than 22 dB. Response time, switch on time, switch off time and recovery time of the switches are lower than 18 ns, 20 ns, 10 ns and 18 ns, respectively. The 118 GHz switch can be used as a protector of the receivers and channel switching device in radiometer or transceiver modules.

1 Circuit configuration and design

Figure 1 shows the schematic diagram of the distributed SPDT switch, which can be seen as composing of two single pole single throw (SPST) circuits. The PIN diodes can be connected by different ways to realize required IL and isolation. Diodes in shunt configuration were commonly adopted at millimeter wave frequency for high-power handling capability and low IL. Disadvantages of shunt configuration are low isolation with the same number of diodes and large circuit dimension with quarter-wavelength between device chips. Devices in series configuration may provide more compact designs with increased IL. In order to reduce the IL of the SPDT switches at 118 GHz, the applied PIN diodes are shunt in configuration. Considering the width of the diode, the devices mounting gap L_1, L_2, L_3 and L_4 lengths are adopted as three-quarter-wavelength at the expense of the switch isolation. The quasi-MMIC SPDT impedance is matched to 50 Ω for integration with other circuit.

The selected beam lead heterojunction PIN diode was fabricated by GaAs foundry of Nanjing Electronic Devices Institute (NEDI). In order to realize low IL and high isolation for the switches, reducing the series resistance of the diode is a very effective way. For the switch circuit in Fig. 1, reducing the diode on-state series resistance provides a low resistivity path to ground for high isolation. Low IL was achieved by tuning out the off-state capacitance with a proper matching network. The device

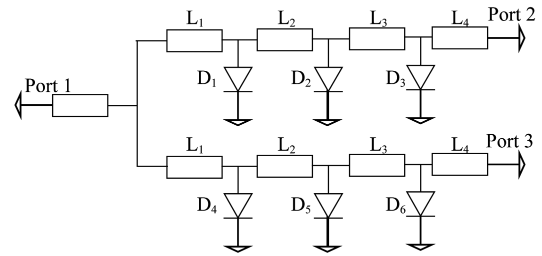

Fig. 1　Schematic of the SPDT switch
图 1　SPDT 开关原理图

was designed as a heterojunction PIN diode to lower series resistance[5-6]. As described in Fig. 2 (a) the cross-section view of GaAs PIN diode, two dissimilar semiconductor materials were applied in P + anode region to create a wide bandgap, the difference in bandgap enabled a suitable barrier height difference which enhances forward injection of holes from the P + anode into the I-region and retards the back injection of electrons from the I-region into the P + anode under forward bias. The result is that the PIN diode has a significantly higher concentration of charge carriers to reduce the RF resistance of the I-region. The capacitance of the diode will remain unchanged since the thickness and resistivity of the I-region are unchanged.

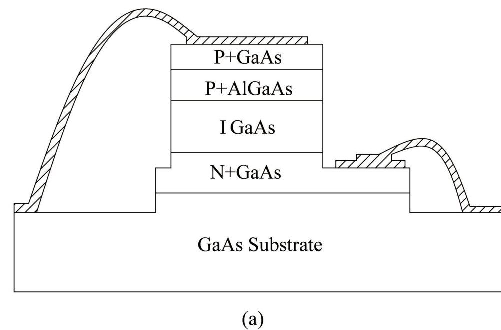

(a)

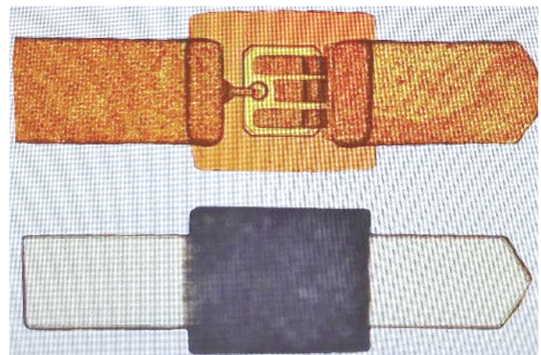

(b)

Fig. 2　AlGaAs/GaAs PIN diode, (a) Cross-section view (b) Photograph
图 2　AlGaAs/GaAs PIN 二极管，(a) 剖面图 (b) 实物照片

The developed GaAs PIN diode is presented in Fig. 2 (b). The thickness of N^+ GaAs is 2 μm with doping concentration of 5×10^{18} cm^{-3}, the thickness of I GaAs is

4 um with doping concentration of 5×10^{14} cm^{-3}, the thickness of P^+ AlGaAs is 0.5 um with doping concentration of 1×10^{19} cm^{-3}, and the thickness of protective layer P^+ GaAs is 0.01 um. The anode contact metal on the P^+ layer is Ti/Pt/Au, and the cathode contact metal on the N^+ layer is Au/Ge/Ni. The measured RF resistance of the diode is shown in Fig. 3 (a), and the forward resistance is 3.5 Ω at 470 MHz with current of 20 mA. Fig. 3(b) shows that the measured total capacitance of the diode is 20 fF at 1 MHz with reverse voltage of 5 V. The PIN diode has the characteristic of low series resistance and low total capacitance which is especially important for the following 118 GHz SPDT switch design.

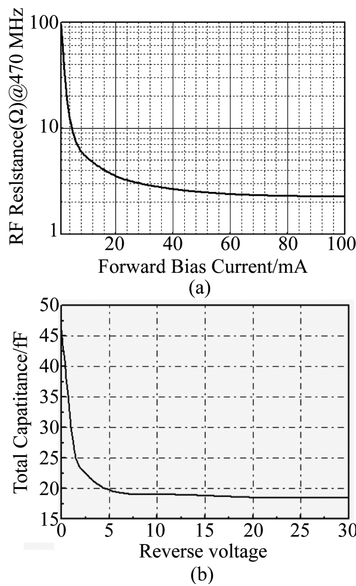

Fig. 3 Measured results of the diode (a) resistance at 470 MHz, (b) total capacitance at 1 MHz
图3 二极管测试数据（a）470 MHz 时电阻（b）1 MHz 时电容

While operating in millimeter wave band, the effect of the GaAs PIN diode parasitic parameters becomes more significant and must be accurately considered in circuit analysis. The equivalent circuit model of the PIN diode is shown in Fig. 4, accurate physical structure of the diode is setup in full-wave EM simulator HFSS[17]. The diode is analyzed with de-embedding method to extract its S-parameters. By fitting S-parameters of the equivalent circuit to the extracted S-parameters in circuit simulator ADS, the extracted parasitic capacitance C_p, zero bias capacitance C_{jo}, parasitic series resistance R_s, and intrinsic on-state resistance R_{on} and off-state resistance R_{off} are shown in Table 1.

As described in Fig. 1, while one channel of the SPDT switch is in on-state, the PIN diodes in this path are reverse biased and are equivalent as an inductor in series with a capacitor . The other channel of the SPDT switch is in off-state, the PIN diodes are positive biased and are equivalent as an inductor in series with a resistor of several ohms. Considering the parasitic inductance of the diode beam lead, equivalent circuit of the SPDT switch in on-state is synthesized as band pass filter (BPF). Figure 5 (a) shows equivalent circuit model of the SPDT distributed switch, in which the diodes in one channel are modeled as on-state and the other channel as off-state. Figure 5 (b) shows the synthesized BPF with Filter Solutions 2009 software. The simulated S-parameters of the BPF are presented in Fig. 5(c), IL is less than 0.3 dB, return loss is better than 15 dB and isolation is higher than 26 dB. Table 2 presents the value of the equivalent circuit lumped elements, in which the parallel inductance, resistor or capacitance are modeled by the on-state or off-state PIN diodes, respectively.

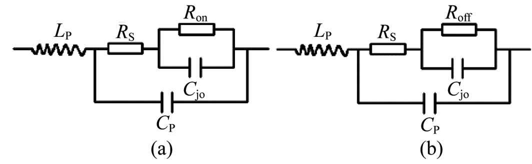

Fig. 4 Equivalent circuit of the diode, (a) on-state (b) off-state
图4 二极管等效电路，(a) 打开状态 (b) 关闭状态

Table 1 Equivalent circuit parameters of the diode
表1 二极管等效电路参数

L_p	C_p	C_{jo}	R_s	R_{on}	R_{off}
0.12 nH	0.017 pF	0.013 pF	3.5 Ω	0.5 Ω	129 kΩ

In Fig. 1, the low impedance microstrip lines L_1, L_2, L_3 and L_4 are designed as three-quarter-wavelength. The lines can be approximated as a capacitor in series with an inductor. For best results, based on the calculated initial width and length parameters of the microstrip lines, a number of iterations have been performed in HFSS. As shown in Fig. 6 (a), the whole switch circuit is setup in HFSS simulator and the diode physical structure is assigned with proper material constants[18]. Advantage of this approach is the elimination of the diode equivalent model extraction from measurement and the circuit can be optimized in HFSS. The simulator can actually model the PIN diodes as long as the material properties such as conductivity, dielectric constant, and dielectric loss are properly assigned at on-state or off-state. The diode physical model parameter values in HFSS are presented in Table 3. The materials are approximated as no losses for fast calculation. The microstrip lines L_1, L_2, L_3 and L_4 are optimized for minimum IL and high isolation, and the input and output impedances are matched to 50 Ω for integration with other circuits. The simulated S-parameters of the SPDT are presented in Fig. 6 (b), IL is less than 2 dB, return loss is better than 11 dB and isolation

Table 2 The value of the equivalent circuit lumped elements
表2 集总元件数值

L_1	C_1	L_2	C_2	L_3	C_3	L_4	C_4	R_5, R_6, R_7	L_5, L_6, L_7	C_5, C_6, C_7
27.2pH	34.7fF	21.5pH	13.3fF	24.6pH	15.6fF	70.2pH	19.7fF	3.5Ω	120pH	30fF

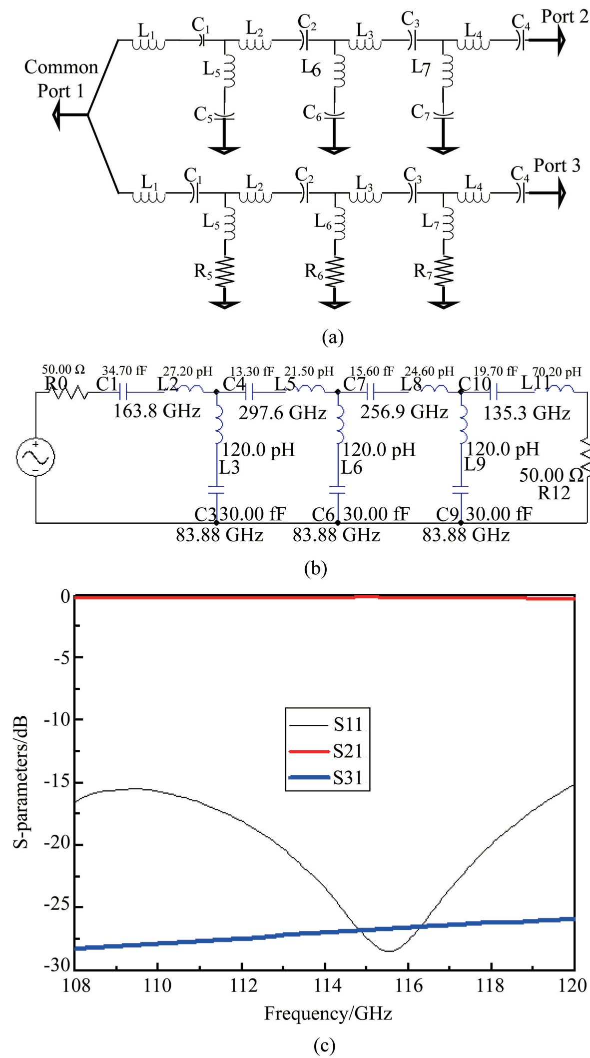

Fig. 5　Synthesized SPDT switch model, (a) equivalent circuit, (b) synthesized BPF, (c) Simulated S-parameters
图 5　综合出的 SPDT 开关模型, (a) 等效电路, (b) 带通滤波器, (c) S 参数仿真数据

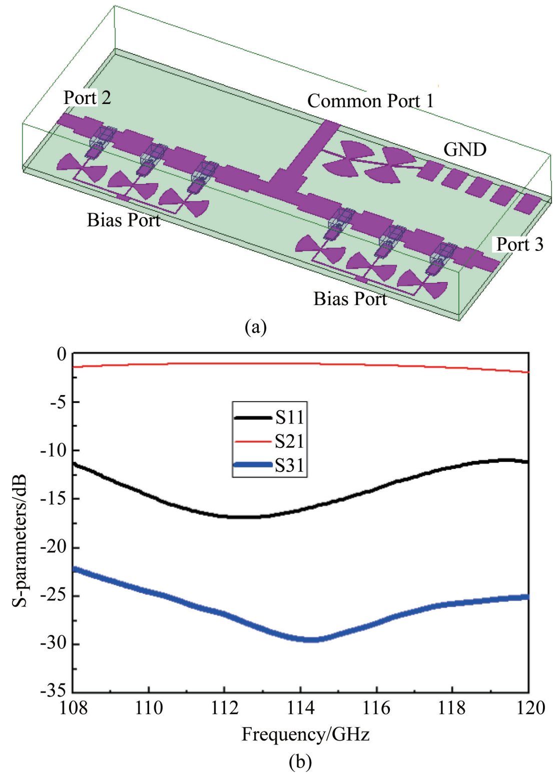

Fig. 6　SPDT physical model, (a) Model in HFSS, (b) Simulated S-parameters
图 6　SPDT 物理模型, (a) HFSS 模型, (b) S 参数仿真数据

is higher than 23 dB.

Table 3　PIN Diode material
表 3　PIN 二极管材料

	Relative permittivity	Dielectric loss tangent	Conductivity/(S/m)
P + Layer	12.9	0	4.1×10^{7}
N + Layer			4.1×10^{7}
I Intrinsic Layer			On-state 2.15×10^{3}
			Off-state 0.25

2　Circuit realization and experiment

The optimized SPDT switch circuit was fabricated on fused quartz substrate with the dielectric constant of 3.78, and thickness of 0.1 mm. As presented in Fig. 7 (a), the circuit is mounted to the split block with silver epoxy, and the PIN diodes are attached to the circuit by thermo-compression bonding. The switch block is manufactured by aluminum and electroplated with gold. The diodes forward DC current was provided by WQD0035H Si CMOS driver chip which was designed by NEDI, and the driver voltage was provided by 7805 and 7905 Si chip with fixed ±5 V output voltage respectively. As the PIN diodes protector, a surface mounted 150 Ω resistor with 0603 package is in series connected between the driver and the switch circuit diodes, the diodes turn-on voltage is 1.1 V and the calculated total current is 26 mA.

2.1　Measurement of the original switches

As described in Fig. 7 (a), the original hybrid integrated SPDT modules connector type is a standard WR-08 rectangular waveguide, and E-plane waveguide to microstrip probe is used for signals transition to planar circuit. Because of the limitation of the quartz circuit sawing technology, the SPDT circuit is sawed as two parts, waveguide to microstrip transition and switch circuit. Gold bonded ribbon is used for connecting the probe transition with the SPDT circuit, in which the transition size is $1.25\times0.65\times0.1$ mm^3 and the SPDT circuit size is $6\times2.5\times0.1$ mm^3. An Agilent N5245A PNA-X network analyzer along with Farran D-band frequency extension modules FEV-06 were used for S-parameters measurement. The measured results were plotted in Fig. 7 (b). The IL results are less than 5.0 dB in the frequency range 110 ~ 120 GHz and its fluctuation is large with the value of 2.5 dB, which is too large and unsuitable for radiometers application. The tested switches total current consumption is 30 mA, and the current flowing through each diode is about 10 mA, which is very close to the calculation.

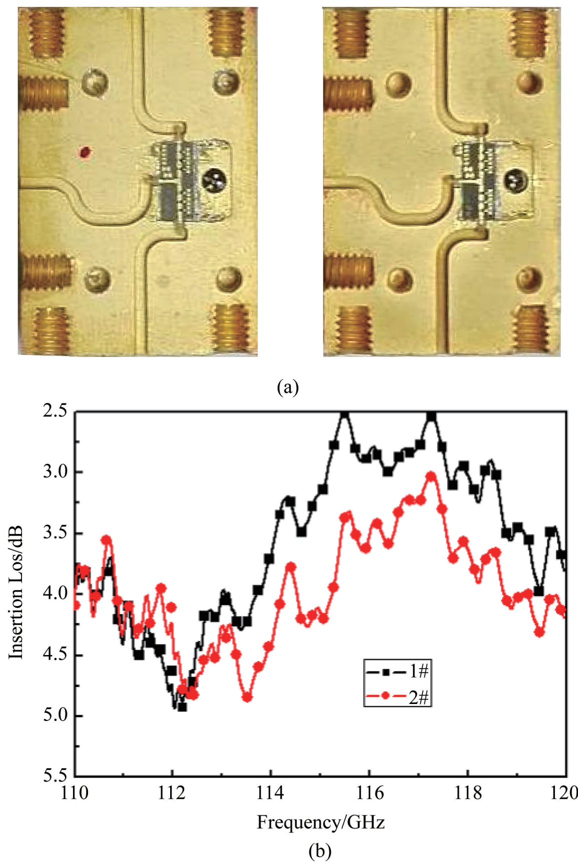

Fig. 7 Original designed switches: (a) photo, (b) measured IL
图 7 最初设计的开关,(a) 实物照片 (b) 插损测试数据

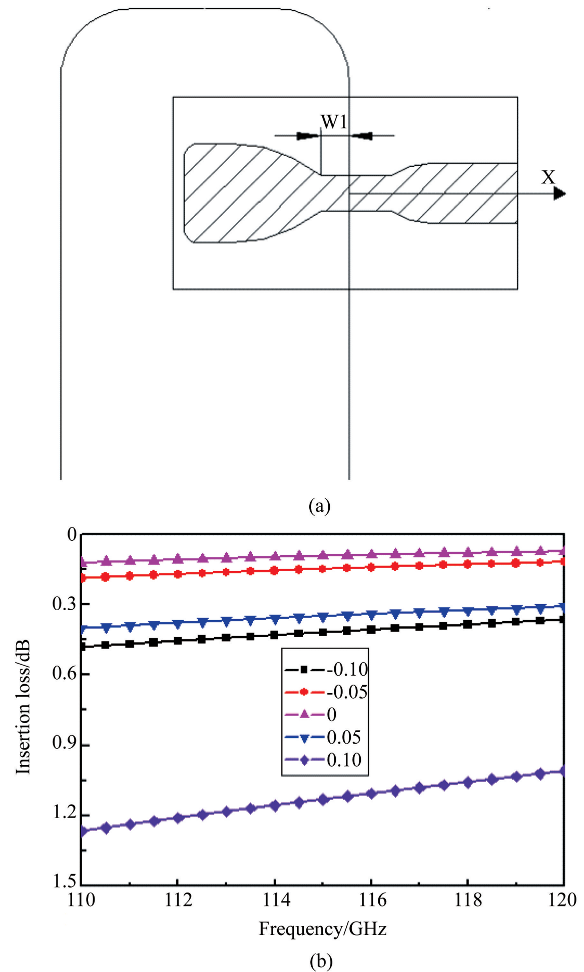

Fig. 8 Waveguide to microstrip E-plane transition, (a) model, (b) simulated IL VS W_1
图 8 波导-微带 E 面过渡,(a) 模型 (b) 插损与 W_1 仿真数据

2.2 IL loss analysis

At millimeter wave frequency band, especially above 100 GHz, the waveguide to microstrip transition and the switch circuit are commonly manufactured as a whole to avoid added IL. The SPDT IL difference between the measurement and simulation is mainly caused by mounted deviation of the transitions and bonded ribbons. As described in Fig. 8 (a), with different deviation value W_1, the effect of transitions on IL is discussed as in Fig. 8 (b), and the results are obvious. While absolute value of the W_1 is higher than 0.05 mm, the added IL increases greatly. Therefore, low IL can be achieved if the transition deviation W_1 value is lower than 0.05 mm.

The bonded ribbon is another reason of IL increasing. As described in Fig. 9 (a), the width of the 50 Ω quartz microstrip is 0.21 mm and the bonded available ribbon width is 0.25 mm. With H_1 = 0.15 mm (the distance from microstrip ground plane to the summit point of the bounding ribbon), G_1 = 0.1 mm, it can be found from Fig. 9 (b) that the IL increases rapidly while the length W_2 is larger than 0.05 mm. Therefore, the W_2 should be kept below 0.05 mm for low IL. In Fig. 9 (c), with W_2 = 0.05 mm, H_1 = 0.15 mm, the IL of the bonded ribbon also increases rapidly while G_1 is wider than 0.1 mm. Therefore, G_1 should be below 0.1 mm. In Fig. 9 (d), IL increases when H_1 is higher than 0.2 mm with W_2 = 0.05 mm and G_1 = 0.1 mm. Therefore, H_1 should be below 0.2 mm.

As described in Fig. 10 (a), IL can be further improved by compensation of the bonded ribbon ground plane. The simulated IL can be improved about 0.1 ~ 0.2 dB while the compensated ground plane height H_2 ranges from 0.025 mm to 0.075 mm as presented in Fig. 10 (b).

From above discussions, for high connecting performance, the bonded parameters like W_2, G_1, H_1 should be lower than 0.05 mm, 0.1 mm, 0.2 mm, respectively. To the original SPDT modules, the added IL is mainly caused by waveguide to microstrip transition mounting deviation. While the transition mounting deviation W_1 value is in the range from −0.05 mm to −0.1 mm, it can be found in Fig. 8 (b) that the input and output transitions will cause the IL doubled to 0.4 ~ 0.8 dB. The added IL discussions will be given more attentions in the following redesigned SPDT modules. These results are instructive for W-band and even higher frequency multi-chip module (MCM) assembly.

2.3 Measurement of the redesigned switches

Three customized SPDT switch modules were rede-

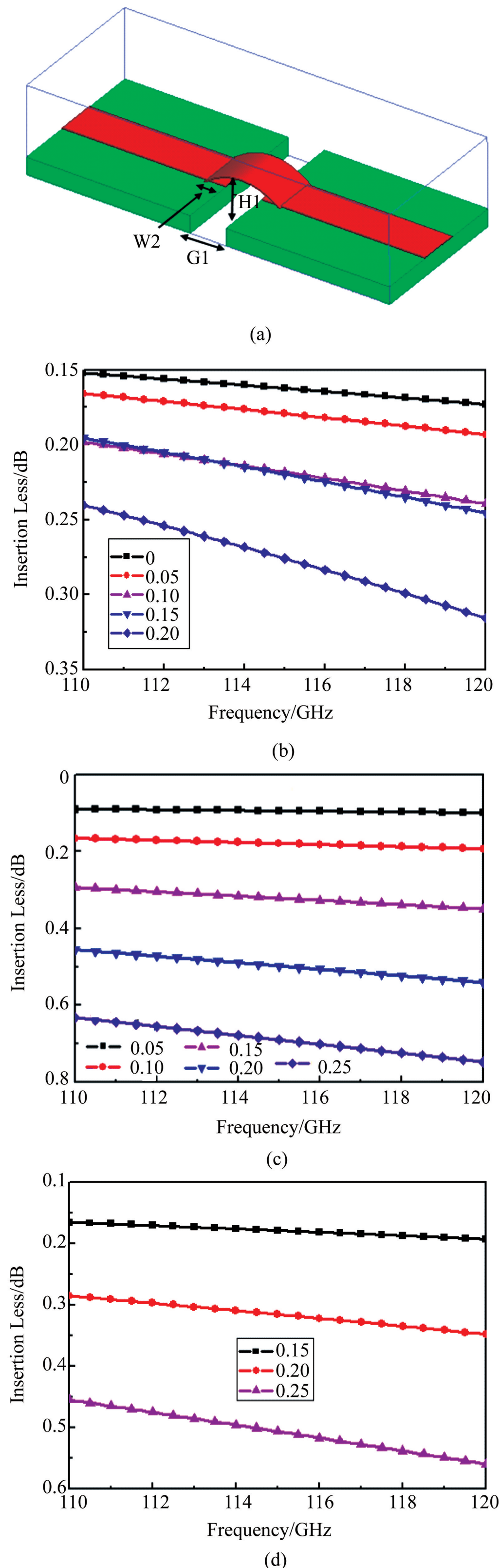

Fig. 9 Bonded ribbon, (a) model, (b) simulated IL vs. W_2, (c) simulated IL vs. G_1, (d) simulated IL vs. H_1

图 9 键合金带,(a) 模型 (b) 插损与 W_2 仿真数据 (c) 插损与 G_1 仿真数据 (d) 插损与 H_1 仿真数据

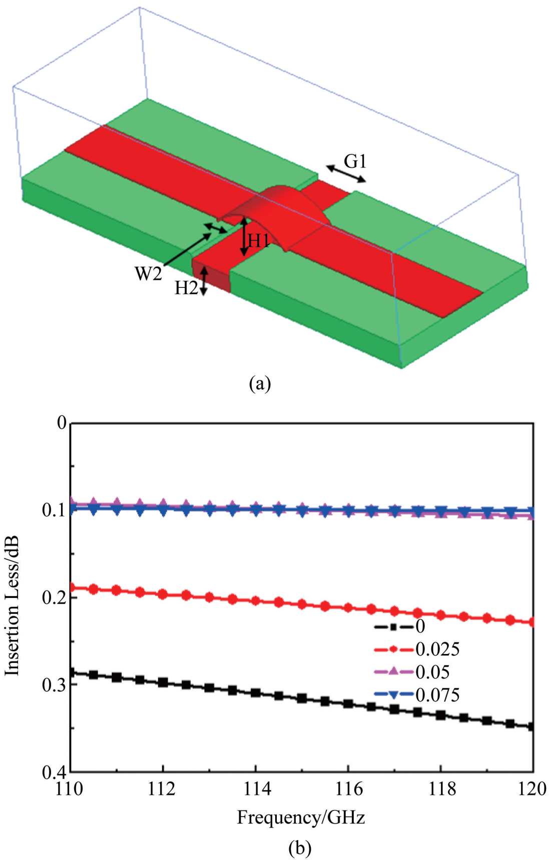

Fig. 10 Bonded ribbon with added ground plane, (a) model, (b) simulated IL vs. H_2

图 10 补偿地的键合金带,(a) 模型 (b) 插损与 H_2 仿真数据

signed as in Fig. 11 (a), one of the switch port is connected with an internally waveguide terminated calibration load. The load material was realized by Eccosorb MF-116 with a 5° taper. This type of compact waveguide load is expected to provide greater than 30 dB of return loss. The switches waveguide port connector type, waveguide to microstrip transition, SPDT circuit, and the tested switch total current consumption are the same as the original designed switches. The measured results of the three switches were plotted in Figs. 11 (b-d). The measured IL results are less than 3.0 dB from 110 to 120 GHz and its typical value is 2.6 dB, and its deviation is low with maximum value of ±0.4 dB. The switches isolation is higher than 22 dB, and the isolation variation trend is the same between the switches. The tested return loss is greater than 13.5 dB. The switch is modulated by the pulse generator 81104 A, the output modulated signal is detected by a self-made detector and then the detected output signal is monitored by Agilent 54622A oscilloscope. In Fig. 11 (e), the switch response time, switch on time, switch off time and recovery time are lower than 18 ns, 20 ns, 10 ns, 18 ns at 118 GHz, respectively.

As described in Table 4, the hybrid integrated SPDT switches feature high frequency and low cost. Subtracting about 1 dB loss of the two waveguide-microstrip transitions, the IL of the designed switches is as low as the MMICs designed with GaAs PIN or SiGe BiCMOS

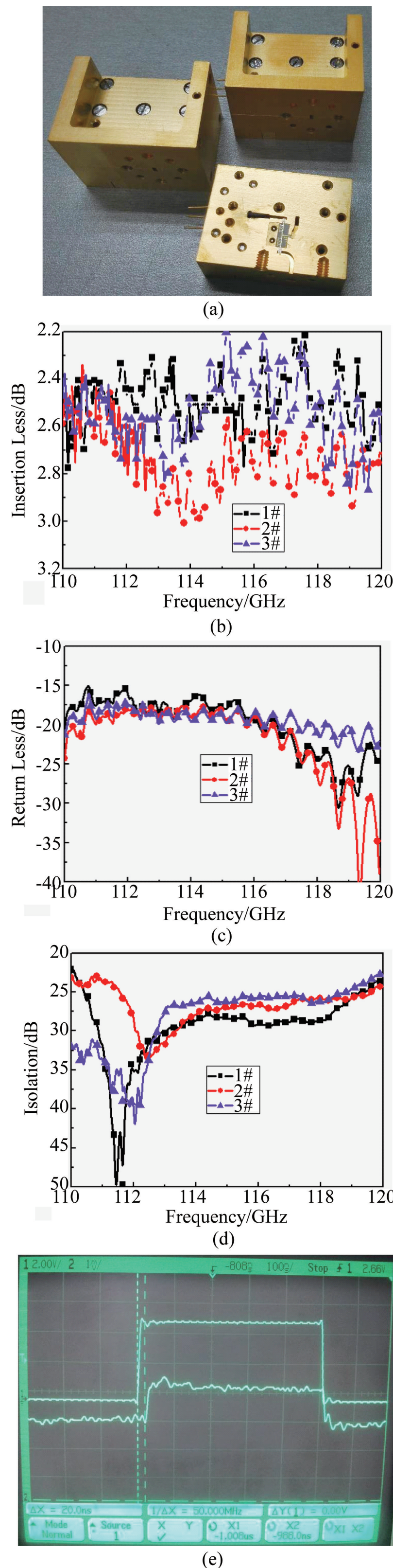

Fig. 11 The customized SPDT switch, (a) photo, (b) measured IL, (c) measured return loss, (d) measured isolation, (e) measured pulse response at 118 GHz
图 11 定制化的 SPDT 开关, (a) 实物照片 (b) 插损测试数据 (c) 回波损耗测试数据 (d) 隔离测试数据 (e) 118GHz 脉冲响应测试数据

technology. It is concluded that if the switches are designed as MMICs, and the diodes gap distance is quarter-wavelength, the isolation and frequency bandwidth of the switches can be further improved.

Table 4 SPDT switches performance comparison
表 4 SPDT 开关性能比较

References	Devices and circuit style	Frequency/GHz	IL/dB	Isolation/dB	Return Loss/dB
This paper	Hybrid circuit modules	110 – 120	2.2 – 3.0	> 22	> 13.5
Ref. [1]	GaAs PIN MMIC	93 – 94	< 1.0	> 30	—
Ref. [9]	GaAs PHEMT MMIC	40 – 85	< 2.0	> 30	—
Ref. [10]	GaAs HEMT MMIC	15 – 80	< 3.6	> 25	—
Ref. [11]	GaAs HEMT MMIC	80 – 100	1.7 – 3.0	32 – 37	8 – 20
Ref. [12]	Si CMOS MMIC	60 – 110	3.0 – 4.0	> 25	> 10
Ref. [13]	SiGe BiCMOS MMIC	82 – 110	< 1.8	> 19.3	> 10
Ref. [14]	SiGe BiCMOS MMIC	73 – 133	1.4 – 2.2	19 – 22	> 10
Ref. [15]	SiGe BiCMOS MMIC	78 – 110	< 1.3	> 22	> 15
Ref. [16]	SiGe BiCMOS MMIC	96 – 163	2.6 – 3.0	23.5 – 29	9 – 15

3 Conclusions

118 GHz SPDT switches are designed with filter synthesis method. Based on equivalent circuit parameters of the AlGaAs/GaAs heterojunction PIN diodes, lumped element filter model of the switch is synthesized and its equivalent distributed circuit is developed. The shunt connected discrete PIN diode provides a low on-state series resistance path to the ground to obtain high isolation. The IL introduced by the mounted waveguide microstrip transition and the bonded ribbons is discussed. The measured IL of the SPDT switch modules is less than 3.0 dB in 110-120 GHz and typical value is 2.6 dB. Their isolation is higher than 22 dB from 110 to 120 GHz. Response time, switch on time, switch off time and recovery time of the switches are lower than 18 ns, 20 ns, 10 ns and 18 ns, respectively. In our future work, optimization of the switch circuits will incorporate with the diodes physical structure, using MMIC technique and adopt the diode gap distance as quarter-wavelength to implement even broader band, lower IL, higher isolation and higher uniformity switches.

References

[1] Putnam J, Fukuda M, Staecker P, *et al.* A 94 GHz monolithic switch with a vertical PIN diode structure [C]. *Gallium Arsenide Integrated Circuit (GaAs IC) Symposium*, 1994, **16**(3):333 – 336.

[2] Alekseev E, Pavlidis D, Dickmann M, *et al.* W-band InGaAs/InP PIN diode monolithic integrated switches [C]. *Gallium Arsenide Integrated Circuit (GaAs IC) Symposium*, 1996:285 – 288.

[3] Case M, Matloubian M, Sun H C, *et al.* High-performance W-band GaAs PIN diode single-pole triple-throw switch CPW MMIC [C]. *Microwave Symposium Digest*. 1997:1047 – 1051.

[4] Buber T, Kinayman N, Hoon Y Y, *et al.* Low-loss high-isolation 60-80 GHz GaAs SPST PIN switch [C]. *IEEE MTT-S International Microwave Symposium Digest*, June, 2003:1307 – 1310.

[5] Rozbicki A, Brogle J, Jain N, *et al.* Ka band high power AlGaAs PIN diode switches [C]. *IEEE MTT-S International Microwave Symposium Digest*, 2009:453 – 456.

[6] Boles T, Brogle J, Hoag D, *et al.* AlGaAs PIN Diode Multi-Octave, mmW Switches [C]. *IEEE International Conference on Microwaves, Communications, Antennas and Electronics Systems*, 2011:1 – 5.

[7] http://www.hxi.com.

[8] http://www.millitech.com.

[9] Kim J Y, Ko W, Kim S H, J. *et al.* A High-Performance 40-85 GHz MMIC SPDT Switch Using FET-Integrated Transmission Line Structure

[J]. *IEEE Transaction on Microwave Wireless and Components. Letters*, 2003, **13**(12):505 – 507.

[10] Lin K Y, Tu W H, Chen P Y, *et al*. Millimeter-Wave MMIC Passive HEMT Switches Using Traveling-Wave Concept [J]. *IEEE Transactions on Microwave Theory and Techniques*, 2004, **52**(8): 1798 – 1808.

[11] http://www.st.northropgrumman.com/mps.

[12] Lai R b, Kuo J J, H. Wang. A 60-110 GHz Transmission-Line Integrated SPDT Switch in 90 nm CMOS Technology [J]. *IEEE Transaction on Microwave Wireless and Components Letters*, 2010, **20**(2):85 – 87.

[13] Schmid R L, Ulusoy A Ç, Song P, *et al*. A 94 GHz 1.4 dB Insertion Loss Single-Pole Double-Throw Switch Using Reverse-Saturated SiGe HBTs [J]. *IEEE Transaction on Microwave Wireless and Components Letters*, 2014, **24**(1):56 – 58.

[14] Song P, Schmid R L, Ulusoy A C, *et al*. A high-power, low-loss W-band SPDT switch using SiGe PIN diodes [C]. *IEEE Radio Frequency Integrated Circuits Symposium*, 2014:195 – 198.

[15] Schmid R L, Song P, Coen C T, *et al*. On the Analysis and Design of Low-Loss Single-Pole Double-Throw W-Band Switches Utilizing Saturated SiGe HBTs [J]. *IEEE Transactions on Microwave Theory and Techniques*, 2014, **62**(11):2755 – 2767.

[16] Ulusoy A Ç, Song P, Schmid R L, *et al*. A Low-Loss and High Isolation D-Band SPDT Switch Utilizing Deep-Saturated SiGe HBTs [J]. *IEEE Transaction on Microwave Wireless and Components Letters*, 2014, **24**(6):400 – 402.

[17] Askari M, Kaabi H, Kavianl Y S. A switched T-attenuator using 0.18 μm CMOS optimized switches for DC-20 GHz [J]. *International Journal of Electronics and Communications*, 2015, **69**:1760 – 1765.

[18] Yao C F, Zhou M, Luo Y S, et al. Research on Millimeter Wave Broad-Band and Low Insertion Loss Limiters Based on Butterworth Low Pass Filter [J]. *ACTA Electronica Sinica*, 2013, **41**(9): 1809 – 1814.

(上接第 518 页)

devices such as III-V MOSFETs, HEMTs, IMOS, and IMPATT diodes in THz field.

References

[1] Hughes S, Citrin D S. Ultrafast heating and switching of a semiconductor optical amplifier using half-cycle terahertz pulses [J]. *Phys. Rev. B*, 1998, **58**(24): 15969 – 15972.

[2] Hirori H, Nagai M, Tanaka K. Excitonic interactions with intense terahertz pulses in ZnSe/ZnMgSSe multiple quantum wells [J]. *Phys. Rev. B*, 2010, **81**(8): 081305.

[3] Hoffmann M C, Monozon B S, Livshits, D, *et al*. Terahertz electro-absorption effect enabling femtosecond all-optical switching in semiconductor quantum dots [J]. *Appl. Phys. Lett.*, 2010, **97**(23): 231108.

[4] Ogawa T, Watanabe S, Minami N, *et al*. Room temperature terahertz electro-optic modulation by excitons in carbon nanotubes [J]. *Appl. Phys. Lett.*, 2010, **97**(4): 041111.

[5] Quinlan S M, Nikroo A, Sherwin M S, *et al*. Photoluminescence from AlxGa1-xAs/GaAs quantum wells quenched by intense far-infrared radiation [J]. *Phys. Rev. B*, 1992, **45**(16): 9428 – 9431.

[6] Orr J M S, Buckle P D, Fearn M, *et al*. Schottky barrier transport in InSb/AlInSb quantum well field effect transistor structures [J]. *Semicond. Sci. Technol.*, 2006, **21**(10):1408 – 1411.

[7] Nash G R, Haigh M K, Hardaway H R, *et al*. InSb/AlInSb quantum-well light-emitting diodes [J]. *Appl. Phys. Lett.*, 2006, **88**(5): 051107.

[8] Hoffmann M C, Hebling J, Hwang H Y, *et al*. THz-pump/THz-probe spectroscopy of semiconductors at high field strengths [J]. *J. Opt. Soc. Am. B*, 2009, **26**(9): 29 – 34.

[9] Wen H, Wiczer M, Lindenberg A M. Ultrafast electron cascades in semiconductors driven by intense femtosecond terahertz pulses [J]. *Phys. Rev. B*, 2008, **78**(12): 125203.

[10] Hoffmann M C, Hebling J, Hwang H Y, *et al*. Impact ionization in InSb probed by terahertz pump-terahertz probe spectroscopy [J]. *Phys. Rev. B*, 2009, **79**(16):161201.

[11] Sharma G, Al-Naib I, Hafez H, *et al*. Carrier density dependence of the nonlinear absorption of intense THz radiation in GaAs [J]. *Opt. Express*, 2012, **20**(16):18016 – 18024.

[12] Su F H, Blanchard F, Sharma G, *et al*. Terahertz pulse induced intervalley scattering in photoexcited GaAs [J]. *Opt. Express*, 2009, **17**(12):9620 – 9629.

[13] Jacoboni C, Reggiani L. The Monte Carlo method for the solution of charge transport in semiconductors with applications to covalent materials [J]. *Rev. Mod. Phys.*, 1983, **55**(3):645 – 705.

[14] Fischetti M V. Monte Carlo simulation of transport in technologically significant semiconductors of the diamond and zinc-blende structures. I. Homogeneous transport [J]. *IEEE Trans. Electron Devices*, 1991, **38**(3):634 – 649.

[15] Chu Z, Liu J, Wang K. Coherent detection of THz waves based on THz-induced time-resolved luminescence quenching in bulk gallium arsenide [J]. *Opt. Lett.*, 2012, **37**(9):1433 – 1435.

[16] Chu Z, Liu J, Liu J. Study of THz-wave-induced photoluminescence quenching in GaAs and CdTe [J]. *Appl. Phys. B*, 2012, **109**:113 – 119.

[17] Lugli P, Bordone P, Reggiani L, *et al*. Monte Carlo studies of nonequilibrium phonon effects in polar semiconductors and quantum wells. I. Laser photoexciation [J]. *Phys Rev B*, 1989, **39**(11):7852 – 7865.

[18] Collins C L, Yu P Y. Nonequilibrium phonon spectroscopy: A new technique for studying intervalley scattering in semiconductors [J]. *Phys Rev B*, 1983, **27**(4):2602 – 2604.

[19] Herbert D C, Childs P A, Abram R A, *et al*. Monte Carlo simulations of high-speed InSb-InAlSb FETs [J]. *IEEE Trans. Electron Devices.*, 2005, **52**(6):1072 – 1078.

[20] Rodilla H, González T, Pardo D, *et al*. High-mobility heterostructures based on InAs and InSb: A Monte Carlo study [J]. *J. Appl. Phys.*, 2009, **105**(11):113705.

[21] Johnston M B, Whittaker D M, Corchia A, *et al*. Simulation of terahertz generation at semiconductor surfaces [J]. *Phys Rev B*, 2002, **65**(16): 165301.

[22] Hoffmann M C, Fülöp J A. Intense ultrashort terahertz pulses: generation and applications [J]. *J. Phys. D: Appl. Phys.*, 2011, **44**(8): 083001.